Research Paper

Defective synaptic plasticity in a model of Coffin–Lowry syndrome is rescued by simultaneously targeting PKA and MAPK pathways

Rong-Yu Liu, Yili Zhang, Paul Smolen, Leonard J. Cleary, and John H. Byrne

Department of Neurobiology and Anatomy, W.M. Keck Center for the Neurobiology of Learning and Memory, McGovern Medical School at the University of Texas Health Science Center at Houston, Houston, Texas 77030, USA

Empirical and computational methods were combined to examine whether individual or dual-drug treatments can restore the deficit in long-term synaptic facilitation (LTF) of the *Aplysia* sensorimotor synapse observed in a cellular model of Coffin–Lowry syndrome (CLS). The model was produced by pharmacological inhibition of p90 ribosomal S6 kinase (RSK) activity. In this model, coapplication of an activator of the mitogen-activated protein kinase (MAPK) isoform ERK and an activator of protein kinase A (PKA) resulted in enhanced phosphorylation of RSK and enhanced LTF to a greater extent than either drug alone and also greater than their additive effects, which is termed synergism. The extent of synergism appeared to depend on another MAPK isoform, p38 MAPK. Inhibition of p38 MAPK facilitated serotonin (5-HT)-induced RSK phosphorylation, indicating that p38 MAPK inhibits activation of RSK. Inhibition of p38 MAPK combined with activation of PKA synergistically activated both ERK and RSK. Our results suggest that cellular models of disorders that affect synaptic plasticity and learning, such as CLS, may constitute a useful strategy to identify candidate drug combinations, and that combining computational models with empirical tests of model predictions can help explain synergism of drug combinations.

[Supplemental material is available for this article.]

Coffin–Lowry syndrome (CLS) is a genetic disorder caused by X-linked mutations in *rsk2* and is characterized by cognitive impairment and craniofacial and skeletal abnormalities (Delaunoy et al. 2006). In mammals, gene deletion studies have shown an essential role for *rsk2* in cognitive functions and learning (Poirier et al. 2007). In several animal models, *rsk2* expresses the p90 isoform of RSK, a downstream effector of the ERK isoform of MAPK, phosphorylating and activating transcription activators such as CREB (Xing et al. 1996, 1998; Finkbeiner et al. 1997; Choi et al. 2011; Rawashdeh et al. 2016). Previous research has shown that memory formation in vertebrates and invertebrates requires CREB activation. For example, an *rsk2*-null mouse model is deficient in several forms of long-term memory and in stimulus-induced CREB phosphorylation (Dufresne et al. 2001; Poirier et al. 2007; Morice et al. 2013). In *Aplysia*, inhibition of RSK activity by the membrane-permeable molecule BI-D1870 (BID) (Sapkota et al. 2007; Fonseca et al. 2011) significantly reduced serotonin (5-HT)-mediated CREB1 phosphorylation, impairing LTF and long-term enhancement of excitability (LTEE) (Liu et al. 2020), two independent cellular mechanisms for memory storage (Mozzachiodi and Byrne 2010). These data suggest that RSK is required for both LTF and LTEE and acts, at least in part, via activation of CREB1. LTF of *Aplysia* synapses may thus constitute a useful cellular model to study mechanisms underlying synaptic plasticity deficits in CLS (Liu et al. 2020). PKA and ERK are also essential for LTF (Mozzachiodi and Byrne 2010; Alberini and Kandel 2014; Byrne and Hawkins 2015) and contribute to the activation of RSK (Liu et al. 2020; Zhang et al. 2021). These findings suggest that pharmacological activation of these kinases may enhance LTF and long-term memory (LTM). Activation in combination may synergistically (supra-additively) enhance LTF and LTM because of complex interactions of kinase cascades critical for LTF and LTM, including feed-forward and feedback loops. Such complexity contributes to nonlinearity of cellular responses to stimuli. Two drugs targeting distinct kinase cascades could activate these auxiliary pathways and produce a nonlinear response to the stimulus, resulting in synergism. Rolipram, a specific inhibitor of cAMP phosphodiesterase 4 (PDE4), activates PKA and improves long-term potentiation (LTP) and LTM in normal rodents and in rodent models of Rubinstein–Taybi syndrome and traumatic brain injury (Bourtchouladze et al. 2003; Titus et al. 2013). When rolipram is combined with the ERK pathway activator NSC295642, weak LTF induced by 1 µM 5-HT is modestly enhanced, indicating the potential advantages of combining manipulations that target the PKA and ERK pathways (Liu et al. 2017). In order to apply this finding to CLS, we used 50 µM 5-HT to produce greater LTF that could then be reduced by RSK inhibition. We demonstrated that combined administration of rolipram and NSC295642 was sufficient to restore LTF, and the two drugs acted synergistically.

Results

NSC295642 and rolipram alone failed to restore impaired LTF

We first examined whether LTF impaired by 2 µM BID can be rescued by NSC295642 or rolipram (Roli) alone. Normal LTF was induced by exposing *Aplysia* sensory neuron–motor neuron

Corresponding author: john.h.byrne@uth.tmc.edu
Article is online at http://www.learnmem.org/cgi/doi/10.1101/lm.053625.122.

(SN-MN) cocultures to five pulses of 5-HT at standard concentration (50 µM; 20-min interstimulus interval [ISIs]) (Montarolo et al. 1986). EPSPs were measured prior to 5-HT treatment (pretest) and 24 h after treatment (posttest) in six groups: (1) 5-HT, (2) BID +5-HT, (3) Roli+5-HT, (4) Roli+BID+5-HT, (5) NSC295642+5-HT, and (6) NSC295642+BID+5-HT (Fig. 1B,C). As shown in Figure 1C, the standard protocol led to a 51% ± 6% (n = 10) increase in EPSP amplitude, whereas BID reduced LTF to 12% ± 8% (n = 9). Roli (0.1 µM) or 0.01 µM NSC295642 alone each produced slight, but not significant, increases in 5-HT-induced LTF. The EPSP increase in the Roli+5-HT group (n = 10) was 62% ± 9% and was 64% ± 6% in the NSC295642+5-HT group (n = 10). Similarly, these two drugs alone slightly enhanced BID-impaired LTF. The EPSP increase in the Roli+BID+5-HT group (n = 9) was 35% ± 10% and was 29% ± 6% in the NSC295642+BID+5-HT group (n = 10). A one-way ANOVA indicated significant overall differences among the groups ($F_{(5,52)}$ = 7.08, P < 0.001). However, post hoc comparisons (SNK) revealed that neither rolipram alone nor NSC295642 alone significantly enhanced LTF (5-HT vs. Roli+5-HT, q = 1.502, P = 0.293; 5-HT vs. NSC295642+5-HT, q = 1.825, P = 0.407). BID significantly reduced not only 5-HT-induced LTF (5-HT vs. BID+5-HT, q = 5.001, P = 0.005), but also the LTF induced by Roli+5-HT (Roli+5-HT vs. Roli+BID+5-HT, q = 3.49, P = 0.044) and by NSC295642+5-HT (NSC295642 + 5-HT vs. NSC295642+BID+5-HT, q = 4.75, P = 0.012). In addition, neither rolipram nor NSC295642 significantly enhanced BID-impaired LTF (BID+5-HT vs. Roli+BID+5-HT, q = 2.892, P = 0.112; BID+5-HT vs. NSC295642+BID+5-HT, q = 2.152, P = 0.134).

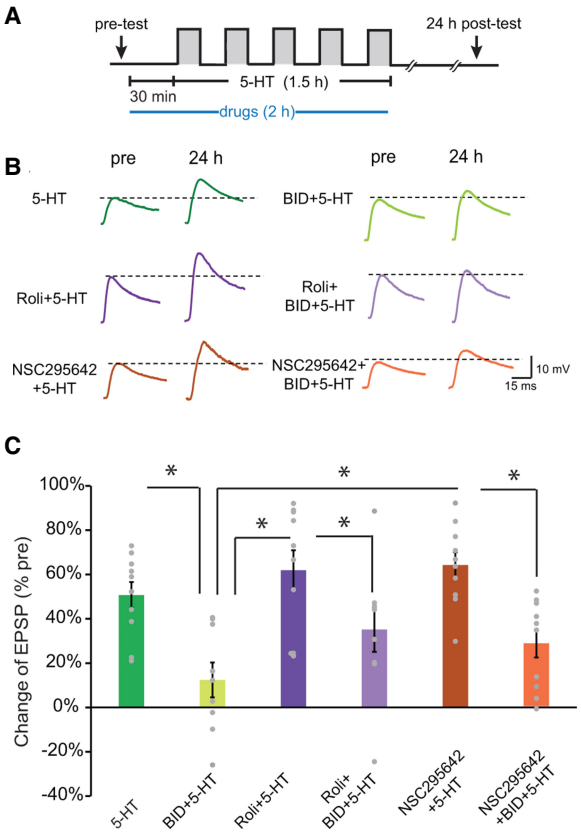

Figure 1. Individual effects of NSC295642 and rolipram on impaired LTF induced by pharmacological inhibition of RSK. (*A*) Protocol for standard five pulses of 50 µM 5-HT treatment in the presence of BID with NSC295642 and/or rolipram (Roli) application. (*B*) Representative EPSPs recorded from MNs in SN-MN cocultures before (Pre) and 24 h after 5-HT treatment. (*C*) Summary data. Inhibition of RSK activity by BID impaired 5-HT-induced LTF. Rolipram alone or NSC 295642 alone did not significantly enhance the facilitation by 5-HT+BID. In this and subsequent illustrations, bar height represents the mean, small bars represent standard error of the mean (SEM), and significant differences are indicated by an asterisk [(*) P < 0.05].

Combining NSC295642 and rolipram rescued LTF

SN-MN cocultures were preincubated with BID in the presence of NSC295642 and/or rolipram for 30 min and then treated with five pulses of 5-HT in continued drug presence (Fig. 1A). Four groups of SN-MN cocultures were assessed: (1) the 5-HT group to assess normal LTF, (2) the BID+5-HT group, (3) the NSC295642 +Roli+5-HT group to assess normal LTF enhanced by combined drugs, and (4) the NSC295642+Roli+BID+5-HT group to assess rescue of LTF by combined drugs (Fig. 2). Standard 5-HT treatment led to a 49% ± 6% (n = 13) increase in EPSP amplitude, whereas BID reduced LTF to 15% ± 6% (n = 11). Combining NSC295642 with rolipram increased normal LTF to 94% ± 13% (n = 9). In the NSC295642+Roli+BID+5-HT group, LTF was enhanced to 100% ± 18% (n = 10). One-way ANOVA indicated significant overall differences among the groups ($F_{(3,39)}$ = 12.69, P < 0.001). Post hoc comparisons (SNK) revealed that LTF in the BID+5-HT group was significantly less than that in the 5-HT group (q = 3.231, P = 0.028). Combined drugs significantly enhanced LTF (NSC295642 +Roli+5-HT vs. 5-HT, q = 4.056, P = 0.007). Importantly, LTF in the NSC295642+Roli+BID+5-HT group was significantly greater than in the 5-HT alone group (q = 4.72, P = 0.005) and was greater than in the BID+5-HT group (q = 7.573, P < 0.001). Moreover, no significant difference in LTF was observed between the NSC295642+Roli+5-HT and NSC295642+Roli+BID+5-HT groups (q = 0.493, P = 0.729). Therefore, comparing Figure 2 with Figure 1, only the combined drugs fully restored LTF.

Previous results suggested that these drugs (0.01 µM NSC295642 with 0.2 µM rolipram) could affect basal synaptic strength (Liu et al. 2017). Therefore, control experiments were performed to examine the extent to which potentiation of LTF could result from EPSP increases due to the drugs without 5-HT. SN-MN cocultures were incubated with 0.01 µM NSC295642 and 0.1 µM rolipram with or without BID for 2 h. EPSP amplitudes with Veh alone did not change significantly at 24 h (−10% ± 3%, n = 7) (Fig. 2B1,B2). BID alone also did not change basal EPSPs significantly (−1% ± 9%, n = 7), nor did NSC295642+Roli (2% ± 10%, n = 7) or NSC295642+Roli+BID (5% ± 8%, n = 7). A one-way ANOVA indicated no significant overall differences among the groups ($F_{(3,24)}$ = 0.721, P = 0.549). Thus, NSC295642 and rolipram did not affect basal synaptic strength. Therefore, the observed enhancement in LTF (Fig. 2A1,A2) was due to the interaction between the PKA and ERK pathways activated by drugs and 5-HT.

Analysis of synergism for the effect of the drug combination on LTF

The above findings that the combined, but not individual, drugs fully rescued BID-impaired LTF suggest that there may be supra-additive (synergistic) effects between ERK activation by NSC295642 and PKA activation by rolipram. The average normal LTF was 51% ± 6% in Figure 1 and 49% ± 6% in Figure 2, and BID-impaired LTF was 12% ± 8% in Figure 1 and 15% ± 6% in Figure 2. Two-sample t-tests indicated the changes in EPSP were not significantly different between the normal ($t_{(1,21)}$ = 0.059, P = 0.81) and BID-impaired ($t_{(1,18)}$ = 0.061, P = 0.81) groups. Therefore, the responses to 5-HT or BID+5-HT in Figures 1 and 2 were combined into a normal LTF group [Fig. 3A, NSC295642(−) Roli(−)] and a BID-impaired LTF group [Fig. 3B, NSC295642(−)

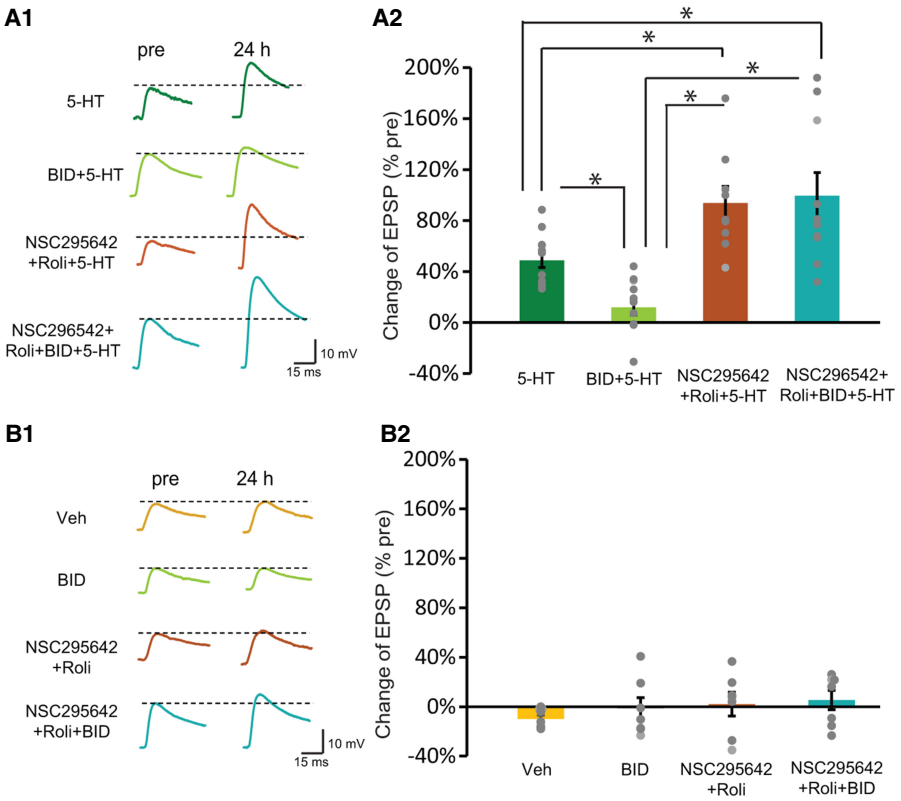

Figure 2. Combined effects of NSC295642 and rolipram on impaired LTF (*A1*,*A2*) and basal EPSPs (*B1*, *B2*). (*A1*) Representative EPSPs recorded from MNs in SN-MN cocultures before (Pre) and 24 h after 5-HT treatment. (*A2*) Summary data. 5-HT-induced LTF was enhanced significantly by coapplying NSC295642 and rolipram but impaired by inhibition of RSK with BID. This impairment was fully rescued by combining NSC295642 and rolipram. (*B1*) Representative EPSPs in absence of 5-HT. (*B2*) Summary data indicate that BID, NSC295642, and rolipram alone or in combination did not change basal synaptic strength.

Roli(−)] to compare individual drug effects versus combination effects. The analysis of normal LTF included four groups: (1) 5-HT, (2) Roli+5-HT, (3) NSC295642+5-HT, and (4) NSC295642+Roli+5-HT. Normal LTF was 50% ± 4% (n = 23) (Fig. 3A, triangle symbol). Rolipram produced a small additional increase to 62% ± 9% (n = 10) (Fig. 3A, square). NSC295642 also caused a small increase to 64% ± 6% (n = 10) (Fig. 3A, asterisk). However, combining NSC295642 and rolipram increased LTF to 94% ± 13% (n = 9) (Fig. 3A, oval).

A number of methods have been introduced to quantitatively assess synergism. We applied the method of Slinker (1998), which has been adopted by multiple groups (Coss et al. 2007; Thackray et al. 2010; Binatti et al. 2021; Ewing et al. 2021; Pantaleon Garcia et al. 2022; Zwolak and Wnuk 2022). With this approach, synergism is assessed by testing the interaction effect in a two-way ANOVA, where the two factors (A and B) are the two drugs of interest, subdivided based on whether the drug is present (+) or absent (−), yielding four groups (A^-B^-, A^+B^-, A^-B^+, and A^+B^+). A two-way ANOVA performed with the data of Figure 3A showed a significant main effect of NSC295642 ($F_{(1,48)}$ = 5.061, P = 0.029) and a trend of an enhanced, but not a statistically significant, effect of rolipram ($F_{(1,48)}$ = 3.954, P = 0.052). More important, no significant interaction between rolipram and NSC295642 ($F_{(1,48)}$ = 1.423, P = 0.239) was observed, indicating an additive but not synergistic interaction between these drugs in their effects on normal LTF.

We next tested for possible synergism of the effects of the two drugs on the rescue of the impaired LTF in the CLS model. The four groups included (1) BID+5-HT, (2) NSC295642+BID+5-HT, (3) Roli+BID+5-HT, and (4) NSC295642 +Roli+BID+5-HT (Fig. 3B). The impaired LTF in BID+5-HT was 14% ± 5% (n = 20) (Fig. 3B, triangle symbol). The application of rolipram produced an increase in LTF to 35% ± 10% (n = 9) (Fig. 3B, square), and NSC295642 increased the LTF to 29% ± 6% in the NSC295642+BID+5-HT group (n = 10). Combining NSC295642 and rolipram with 5-HT increased LTF to 99% ± 18% (n = 10) (Fig. 3B, oval). A two-way ANOVA revealed that the enhancements from rolipram or NSC295642 alone were both significant (factor Roli, $F_{(1,45)}$ = 21.49, P < 0.001; factor NSC295642, $F_{(1,45)}$ = 16.05, P < 0.001). Importantly, the interaction between these two drugs was also significant ($F_{(1,45)}$ = 6.159, P = 0.017), confirming that addition of the two drugs together has a synergistic effect to rescue LTF.

Combined drugs synergistically activated RSK

We investigated molecular mechanisms that may explain, at least in part, this combined-drug synergism. As discussed above, PKA and ERK both activate RSK (Zhang et al. 2021). Therefore, the synergistic effect of the drugs on LTF may be due to synergistic enhancement of RSK phosphorylation. To test this hypothesis, we measured levels of phosphorylated RSK (pRSK) with immunofluorescence. Rolipram and/or NSC295642 was applied with 5-HT to isolated SNs, and RSK phosphorylation was assessed 1 h after 5-HT treatment (Fig. 4A). pRSK levels in the 5-HT, Roli+5-HT, NSC295642 +5-HT, and Roli+NSC295642+5-HT groups were normalized to the group treated with vehicle control. Compared with Veh, 5-HT led to a 23% ± 7% increase in pRSK. The increase of pRSK levels in the Roli+5-HT and NSC295642+5-HT groups was 21% ± 4% and 18% ± 4%, respectively. However, the increase of pRSK in NSC295642+Roli+5-HT was 55% ± 10% (Fig. 4B1–B3). One-way ANOVA indicated significant overall differences among the groups ($F_{(3,21)}$ = 7.59, P = 0.001). Post hoc analysis indicated the pRSK level in NSC295642+Roli+5-HT was significantly greater than in the other groups (NSC295642+Roli+5-HT vs. 5-HT, q = 4.83, P = 0.003; NSC295642+Roli+5-HT vs. Roli+5-HT, q = 5.49, P = 0.002; NSC295642+Roli+5-HT vs. NSC295642+5-HT, q = 6.06, P = 0.002). No significant difference in pRSK was observed between NSC295642+5-HT and 5-HT (q = 0.77, P = 0.855) or between Roli +5-HT and 5-HT (q = 0.228, P = 0.87). To examine whether the dual-drug interaction was synergistic, a two-way ANOVA was performed on the 5-HT, Roli+5-HT, NSC295642+5-HT, and Roli+NSC295642 +5-HT groups. The analysis revealed a significant ($F_{(1,21)}$ = 9.42, P = 0.006) interaction between rolipram and NSC295642 (Fig. 4B3), indicating a synergistic enhancement of the 5-HT-induced increase in pRSK.

Next, we investigated possible synergism between rolipram and NSC295642 in restoring 5-HT-induced pRSK impaired by

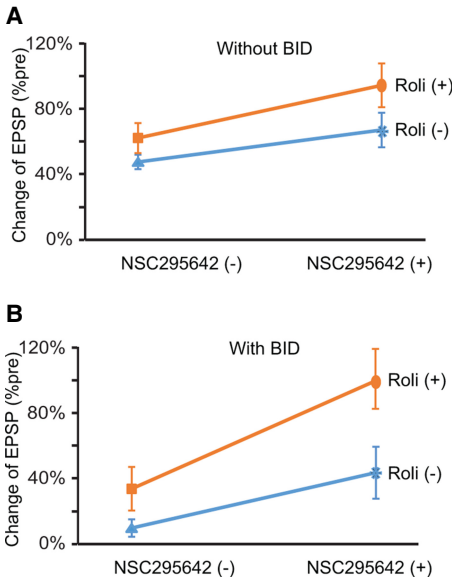

Figure 3. Tests of synergism for the drug combination using the data from Figures 1 and 2. (*A*) Effects of NSC295642 and rolipram on LTF in the absence of BID. Statistical analysis using two-way ANOVA revealed no significant interaction between the groups and therefore a lack of synergism between NSC295642 and rolipram on normal LTF. (*B*) Drug effects on BID-impaired LTF. Statistical analysis using two-way ANOVA revealed a significant interaction between rolipram and NSC295642, indicating synergistic rescue of impaired LTF.

BID. Rolipram and/or NSC295642 was applied to isolated SNs in the presence of BID, and the effects on RSK phosphorylation were examined 1 h after 5-HT treatment (Fig. 4C1–C3). Immunoreactivities to pRSK in the BID+5-HT, Roli+BID+5-HT, NSC295642+BID+5-HT, and Roli+NSC295642+BID+5-HT groups were normalized to vehicle control. Compared with Veh, in the presence of BID, 5-HT yielded no significant change in pRSK (5% ± 4%). The changes in pRSK in the Roli+BID+5-HT and NSC295642+BID+5-HT groups was 11% ± 4% and 10% ± 6% of control, respectively. However, the increase of pRSK in Roli +NSC295642+BID+5-HT was 42% ± 5% of control. One-way ANOVA indicated significant overall differences among the groups ($F_{(3,31)} = 11.49$, $P < 0.001$). Post hoc comparison indicated pRSK in the NSC295642+Roli+BID+5-HT group was significantly greater than in the other groups (NSC295642+Roli+BID+5-HT vs. BID +5-HT, $q = 7.43$, $P < 0.001$; NSC295642+Roli+BID+5-HT vs. Roli +BID+5-HT, $q = 6.46$, $P < 0.001$; NSC295642+Roli+BID+5-HT vs. NSC295642+BID+5-HT, $q = 6.53$, $P < 0.001$). Moreover, no significant difference in pRSK was observed between the NSC295642 +BID+5-HT and BID+5-HT groups ($q = 0.922$, $P = 0.519$) or between the Roli+BID+5-HT and BID+5-HT groups ($q = 1.0$, $P = 0.761$).

To determine whether the dual-drug interaction was synergistic, a two-way ANOVA was performed on the BID+5-HT, Roli+BID +5-HT, NSC295642+BID+5-HT, and Roli+NSC295642+BID+5-HT groups. This analysis revealed a significant ($F_{(1,32)} = 9.05$, $P = 0.005$) interaction between rolipram and NSC295642 (Fig. 4C3), indicating a synergistic enhancement of the BID-impaired increase in pRSK.

Computational modeling of synergism

We used a previously developed computational model (Zhang et al. 2021) of the signaling cascades underlying LTF to gain additional insights into the mechanisms of synergism. Figure 5A is a simplified version of the molecular network, focusing on the roles and interactions of the PKA and MAPK cascades. PKA indirectly activates the ERK–RSK cascade (Fig. 5A, pathways 10, 3 → 6 → 7; Zhang et al. 2021). Therefore, enhancing the activity of the PKA pathway by drugs such as rolipram will also enhance the activity of the ERK–RSK pathway. PKA also indirectly activates RSK by an ERK-independent pathway, forming a positive feedforward loop (Fig. 5A, pathways 10, 3 → 6 → 7; Zhang et al. 2021). Thus, it is plausible that some combinations of drugs that individually activate these PKA and ERK pathways would take advantage of the nonlinear interactions between these pathways to act synergistically.

Due to the lack of dose response curves for NSC295642/rolipram concentrations versus the enhancement of ERK/PKA activity and of a dose response curve for BID concentration versus the suppression of downstream effects of RSK, the model could not simulate the effects or predict the synergism of specific drug concentrations used in this study. Therefore, to gain qualitative insights into the molecular determinants of synergism, we ran simulations in a more generalized manner, varying the activation of individual pathways individually or in combination and evaluating their effects on LTF. We denoted the simulated treatment to enhance activation of the PKA pathway as "PKA enhancer;" the treatment to enhance the ERK pathway as "ERK enhancer;" and the treatment to suppress RSK effectors as "RSK inhibitor."

Model equations and parameters describing the PKA and MAPK pathways and their interactions remain as in Zhang et al. (2021) (see the Supplemental Material, Eqs. 1–38; Supplemental Table S1). However, to simulate LTF, the synthesis and activation of the transcription factor CCAAT enhancer binding protein (C/EBP) were added (Fig. 5A, pathways 11, 16–17; Supplemental Material, Eqs. 39–41), given that C/EBP activation is essential for LTF (Alberini et al. 1994; Guan et al. 2002, 2003; Mohamed et al. 2005). The expression of C/EBP is regulated by CREB1 and CREB2 (Fig. 5A, pathways 16–17), and C/EBP is activated by active, phosphorylated ERK (pERK) (Fig. 5A, pathway 11). The peak level of active, phosphorylated C/EBP (pC/EBP) was used as a proxy for the strength of LTF. The effects of RSK inhibition were represented by reducing the effects of RSK on CREB1 and p38 MAPK by 40%–60% (i.e., suppressing pathways 8 and 13 in Fig. 5A; $k_{f,p38\_RSK}$ in Supplemental Material, Eq. 24, and $k_{RSK,CREB1}$ in Supplemental Material, Eq. 28). The effect of PKA activation by rolipram was represented by reducing the degradation rate of the upstream activator of PKA, cyclic AMP (cAMP) ($k_{b,camp}$ in Supplemental Material, Eq. 11). ERK activation by NSC295462 was represented by reducing the deactivation rate of ERK ($k_{b,ERK}$ in Supplemental Material, Eqs. 6,7).

Because the model is deterministic, statistical approaches are not needed to assess simulated synergism. Consequently, synergism of the combined drugs was calculated as follows: Synergism = $\text{Effects}_{\text{combined – drugs}} - (\text{Effects}_{\text{PKA enhancer}} + \text{Effects}_{\text{ERK enhancer}})$.

The variables "effects" represent the increases of pERK, pRSK, or pC/EBP due to treatment by drugs and 5-HT compared with 5-HT treatment only. Because PKA activation will indirectly activate ERK and RSK (Fig. 5A), we predicted that activation of PKA and ERK together will induce synergism at the level of ERK. Moreover, we predicted that as the downstream substrate of ERK, the synergism of RSK will be similar to that of ERK.

$\text{Effects}_{\text{PKA enhancer}} + \text{Effects}_{\text{ERK enhancer}}$ is the value of the additive effect expected if PKA and ERK activators act independently. We therefore assumed that these combined drugs have synergistic effects as long as the value of the variable "synergism" is >0 in the model, although a synergism of low value (e.g., <10%) might not be detectable in empirical studies. A larger value of synergism represents stronger synergism.

To simulate different degrees of ERK activation, we decreased the dephosphorylation rate constant $k_{b,ERK}$ by steps of 1.2%, from

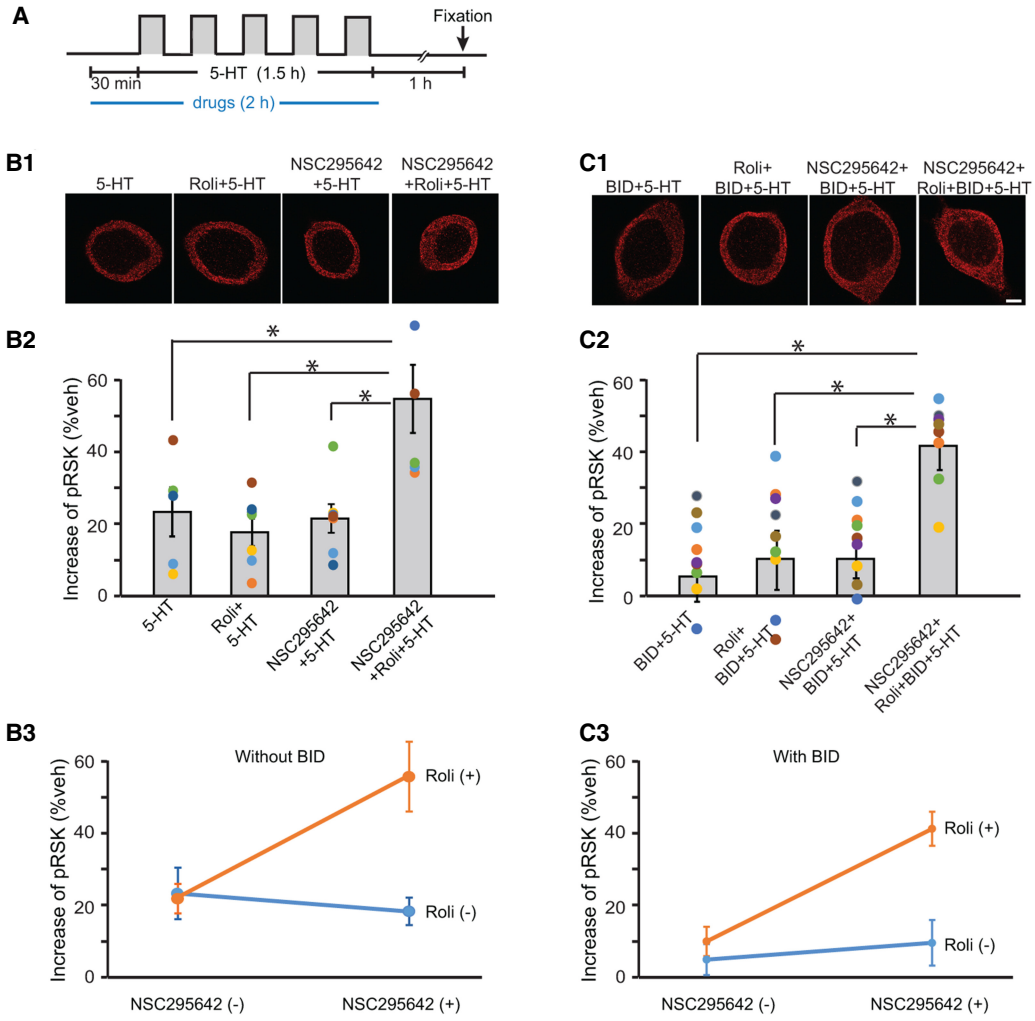

Figure 4. Effects on RSK activation of individual and combined drugs. (*A*) Protocol for standard five pulses of 50 µM 5-HT treatment with NSC295642 and/or rolipram application, without (*B1–B3*) or with (*C1–C3*) BID. (*B1–B3*) Without BID. (*B1*) Representative confocal images of pRSK in SNs 1 h after 5-HT treatment with a single drug or combined drugs. Scale bar, 20 µm. (*B2*) Summary data. Dual drugs potentiated the 5-HT-induced increase in pRSK. (*B3*) Two-way ANOVA indicated a synergism between rolipram and NSC295642. (*C1–C3*) With BID. (*C1*) Representative confocal images of pRSK in SNs 1 h after 5-HT treatment with a single drug or combined drugs. (*C2*) Summary data. Single drugs did not restore pRSK, whereas dual drugs substantially increased 5-HT-induced, BID-impaired pRSK. (*C3*) Two-way ANOVA revealed a synergistic interaction between NSC295642 and rolipram. Different-colored dots in each group indicate individual experiments, and the same color in different groups represents one experiment. Scale bar, 20 µm.

100% down to ~90% of its standard value (Supplemental Table S1). For rolipram, we similarly decreased the degradation rate constant $k_{b,camp}$ by steps of 2.5%, from 100% to ~75% of its standard value (Supplemental Table S1). These small changes of $k_{b,ERK}$ and $k_{b,camp}$ were simulated to be consistent with the empirical findings that NSC+5-HT or Roli+5-HT did not significantly increase pRSK at 1 h after 5-HT compared with 5-HT alone (Figs. 4B2, 6C2). These minor changes of $k_{b,ERK}$ or $k_{b,camp}$ alone did not increase pRSK at 1 h after 5-HT treatment >10% above pRSK induced by 5-HT alone.

The effect of each drug "pair" was simulated for a total of 100 combinations: 10 levels of $k_{b,ERK}$ reduction combined with 10 levels of $k_{b,camp}$ reduction. The *X*-axes and *Y*-axes in Figure 5, B1, B2, and C, denote the percentages of the standard values of these parameters. The *Z*-axes show the synergism variable. In the absence of RSK inhibitor, all combinations of treatments induced a pRSK synergism value near 5%; thus, the combined drugs can increase pRSK ~5% more than the sum of individual drug effects (i.e., weak synergism) (Fig. 5B1). We used the combination that produced the highest synergism for further simulations, which is an ~10% $k_{b,ERK}$ reduction combined with ~25% $k_{b,camp}$ reduction, denoted as "PKA enhancer and ERK enhancer" (indicated by circle in Fig. 5B1). In the absence of RSK inhibition, "PKA enhancer and ERK enhancer" induced a synergism value of −11% in the peak of pC/EBP, the proxy for the strength of LTF (Liu et al. 2013), and a synergism value of 4% in pERK (Fig. 5D1). The negative value shows that the weak synergism in pRSK induced by "PKA enhancer and ERK enhancer" failed to induce synergism in pC/EBP.

The effect of RSK inhibition was represented by reducing the effects of RSK on CREB1 and p38 MAPK by 40%–60% ($k_{f,p38\_RSK}$ in Supplemental Material, Eq. 24, and $k_{RSK,CREB1}$ in Supplemental Material, Eq. 28). With a reduction of 60%, "PKA enhancer and ERK enhancer" (indicated by circle in Fig. 5B2) induced synergism values of 9% in pRSK (Fig. 5B2), 8% in pERK, and 11% in pC/EBP (Fig. 5D1). Similar results were obtained by 40% or 50% reductions. Thus, simulated RSK inhibition increased the synergism in pRSK and pERK and switched the negative synergism of pC/EBP to positive. These results suggest that (1) the synergism values of pERK and pRSK are close in both the presence and absence of RSK

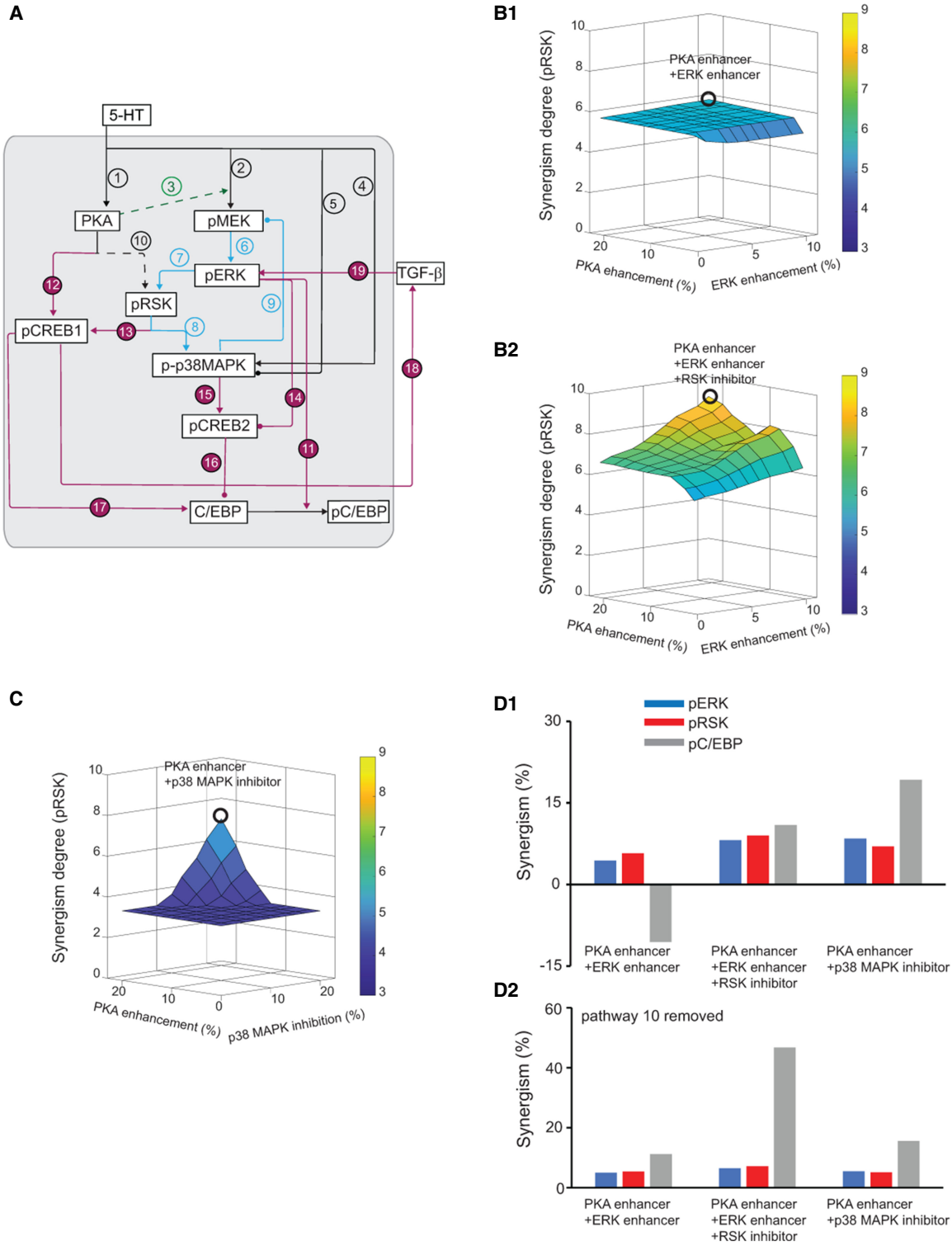

Figure 5. Computational modeling of synergism. (*A*) Schematic model for the molecular network of LTF, simplified from Zhang et al. (2021). The PKA and MAPK cascades interact to regulate the phosphorylation and activities of RSK. PKA, ERK, and RSK in turn regulate the phosphorylation and activation of CREB1 and CREB2. These effects on CREB1 and CREB2 induce the expression of immediate–early genes such as C/EBP. p38 MAPK is activated downstream from RSK; in a negative feedback loop, p38 MAPK inhibits the activation of MEK and therefore of ERK and RSK. Arrows indicate activation, and circular ends indicate repression. Dashed lines represent simplifications of complex cascades that omit intermediate elements. (*B1*,*B2*) 3D plots of synergism in pRSK induced by combined effects of PKA activation (via cAMP phosphodiesterase inhibition) and ERK activation (via reduction of ERK dephosphorylation) in the absence (*B1*) or presence (*B2*) of RSK inhibition. (*C*) 3D plot of synergism in pRSK induced by combined p38 MAPK inhibition and PKA activation. (*D1*,*D2*) Comparison of synergism in pRSK (blue) and pC/EBP (orange) in different treatment combinations (examples indicated by circles in *B1*, *B2*, and *C*) in the presence (*D1*) or absence (*D2*) of pathway 10.

inhibitors. Thus, synergism might occur at both levels. (2) The simulated synergism values of pERK and pRSK in the presence or absence of RSK inhibitors were <10%. (3) At the level of pC/EBP, with the addition of RSK inhibitor, synergism switched from negative to positive values, consistent with the empirical findings that synergism in the change of EPSP was only found in the presence of BID (Fig. 3).

The model suggests further insight into the lack of synergism in LTF. Increased pRSK leads to increased p38 MAPK activity (Fig. 5A, pathway 8). As shown in Figure 5A (pathways $6 \rightarrow 7 \rightarrow 8 \rightarrow 9$) and based on empirical findings from our laboratory (Zhang et al. 2017, 2021), the model includes a negative feedback loop in which RSK, activated by pERK, leads to p38 MAPK activation, which in turn inhibits activation of MEK and ERK, potentially limiting the extent of 5-HT-induced RSK activation and LTF. More importantly, this indirect activation of p38 MAPK due to "PKA enhancer and ERK enhancer" can activate the transcription inhibitor CREB2 (Fig. 5A, pathway 15), leading to decreased expression of C/EBP (Fig. 5A, pathway 16). These effects together can explain why "PKA enhancer and ERK enhancer" leads to a weak synergism of pERK/pRSK and a negative synergism value in pC/EBP (Fig. 5D1), consistent with empirical results (Figs. 3, 4). The addition of RSK inhibitor to suppress activation of p38 MAPK by pRSK (Fig. 5A, pathway 8) may decrease p38 MAPK, subsequently decreasing the activity of CREB2. Thus, "PKA enhancer and ERK enhancer" plus RSK inhibitor produces a positive synergism value in pC/EBP (Fig. 5D1), consistent with the synergism of LTF in Figure 3B.

Therefore, we predicted that an alternative drug combination to induce synergism might be a PKA activator together with an inhibitor of p38 MAPK. A p38 MAPK inhibitor could relieve the inhibition of pRSK and activation of CREB2 by p38 MAPK without affecting the activation of CREB1 by pRSK. To computationally test this hypothesis, we simulated the combined effects of p38 MAPK inhibition and PKA activation on pRSK and pC/EBP. To simulate p38 MAPK inhibition, we gradually decreased the downstream effects of p38 MAPK on MEK and CREB2 (i.e., suppressing pathways 9 and 15 in Fig. 5A; $k_{EP38,\ MEK}$ in Supplemental Material, Eq. 10, and $k_{p38,CREB2}$ in Supplemental Material, Eq. 31) by steps of 2.5%, from 100% down to ~75% of the standard values (see Supplemental Table S1). These minor changes of $k_{EP38,\ MEK}$ do not increase simulated pRSK 1 h after 5-HT treatment >10% above pRSK induced by 5-HT alone. At the same time, we gradually decreased the degradation rate constant of cAMP by steps of 2.5%, from 100% down to ~75% of the standard values. Supporting the new prediction, simulations of these 100 pairs of parameter changes showed that combined p38 MAPK inhibition and $k_{b,camp}$ reduction induced synergism in pRSK (Fig. 5C). We used the combination that produced the greatest synergism for further simulations, which was ~25% p38 MAPK effect reduction combined with ~25% $k_{b,camp}$ reduction, denoted as "p38 MAPK inhibitor and PKA enhancer" (indicated by circle in Fig. 5C). Figure 5D1 shows that "p38 MAPK inhibitor and PKA enhancer" induced synergism values of 7% in pRSK, 8% in pERK, and 19% in pC/EBP. These results predict that an inhibitor of p38 MAPK in combination with PKA activation will enhance normal LTF.

Our previous study suggests that pRSK increases immediately after one pulse of 5-HT, a time when pERK remains at the basal level (Zhang et al. 2021). This immediate increase of pRSK can be blocked by PKA inhibition. These results suggest that PKA activates RSK via an ERK-independent pathway. However, our antibody recognizes pRSK at Thr573, which is a specific phosphorylation site for ERK and not for PKA. Therefore, the PKA effect cannot be direct. One possibility is that a phosphatase targeting Thr573 is inhibited downstream from PKA activation. To investigate whether pathway $3 \rightarrow 6 \rightarrow 7$ alone is sufficient for the synergism of pERK and pRSK, we repeated the simulation of Figure 5D1 after removing pathway 10. Figure 5D2 shows that in the absence of pathway 10, "PKA enhancer and ERK enhancer" induced synergism values of 5% in pRSK and pERK and 11% in pC/EBP. "PKA enhancer and ERK enhancer and RSK inhibition" induced synergisms values of 7% in pRSK, 6% in pERK, and 47% in pC/EBP (Fig. 5D2). "p38 MAPK inhibitor and PKA enhancer" induced synergism values of 5% in pRSK and pERK and 15% in pC/EBP. Thus, pathway $3 \rightarrow 6 \rightarrow 7$ alone is sufficient for simulated synergism. However, removing pathway 10 decreased synergism in pRSK but increased synergism in pC/EBP, suggesting that pathway 10 also plays a role in the synergism. These mixed effects might also be due in part to the pathway ERK–RSK–p38 MAPK in Figure 5A (pathways $6 \rightarrow 7 \rightarrow 8 \rightarrow 9$). Pathway 10 activates RSK, thus increasing the synergism in pRSK. Enhanced pRSK in turn also activates more p38 MAPK, which in turn activates CREB2, suppressing the synergism in pC/EBP.

Activation of PKA and inhibition of p38 MAPK synergistically enhanced ERK and RSK activation

We empirically tested the model prediction (Fig. 5) that p38 MAPK activation can limit the extent of 5-HT-induced RSK activation. Immunostaining for pRSK was performed 1 h after standard 5-HT treatment in the presence of the p38 MAPK inhibitor SB203580 (SB) (Fig. 6A,B1,B2). pRSK levels in the 5-HT, SB, and SB+5-HT groups were normalized to the group treated with vehicle control. Compared with Veh, 5-HT led to a 15% ± 3% increase in pRSK. SB itself produced little change (−5% ± 4%). However, pRSK increased to 25% ± 4% of control in the SB+5-HT group. One-way ANOVA indicated significant overall differences among the treatment groups ($F_{(2,21)} = 16.90$, $P < 0.001$). Post hoc comparisons (SNK) revealed that 5-HT induced significant increases in pRSK (5-HT vs. SB, $q = 5.37$, $P = 0.001$; SB+5-HT vs. SB, $q = 8.08$, $P < 0.001$). There was a trend of significant difference between the SB+5-HT group and the 5-HT group ($q = 2.71$, $P = 0.069$), indicating SB has the potential to enhance the activation of RSK.

Modeling supported the hypothesis that coapplication of a PKA activator and a p38 MAPK inhibitor would synergistically enhance ERK and RSK phosphorylation (Fig. 5C). We therefore tested this hypothesis empirically. Rolipram and/or SB was applied to isolated SNs, and the effects on RSK phosphorylation were examined 1 h after 5-HT treatment. Immunoreactivities to pRSK in the 5-HT, Roli+5-HT, SB+5-HT, and Roli+SB+5-HT groups were normalized to vehicle control (Fig. 6C1). Compared with Veh, 5-HT led to a 19% ± 4% increase in pRSK. The increase in pRSK for Roli+5-HT and SB +5-HT was 25% ± 6% and 26% ± 5% of control, respectively. The increase of pRSK in the combined-drug group was 56% ± 8% of control (Fig. 6C2). One-way ANOVA indicated significant overall differences among the groups ($F_{(3,31)} = 12.52$, $P < 0.001$). Post hoc comparisons (SNK) revealed the combined drugs induced a significant increase in pRSK compared with the other three groups (SB +Roli+5-HT vs. 5-HT, $q = 8.20$, $P < 0.001$; SB+Roli+5-HT vs. SB +5-HT, $q = 6.57$, $P < 0.001$; SB+Roli+5-HT vs. Roli+5-HT, $q = 5.91$, $P < 0.001$), without significant effects from either SB or rolipram on 5-HT-induced pRSK (SB+5-HT vs. 5-HT, $q = 1.68$, $P = 0.245$; Roli +5-HT vs. 5-HT, $q = 2.36$, $P = 0.232$). Importantly, the interaction between rolipram and SB on pRSK was significant (two-way ANOVA, $F_{(1,31)} = 4.75$, $P = 0.038$) (Fig. 6C3), indicating the drug combination of SB and rolipram synergistically increased 5-HT-induced phosphorylation of RSK.

Finally, we tested the potential synergism in pERK induced by a PKA activator and a p38 MAPK inhibitor. Immunoreactivities to pERK in the 5-HT, Roli+5-HT, SB+5-HT, and Roli+SB+5-HT groups were normalized to vehicle control (Fig. 6D1). Compared with Veh, 5-HT led to a 20% ± 4% increase in pERK. The increase in pERK for Roli+5-HT and SB+5-HT was 21% ± 9% and 17% ± 4% of control,

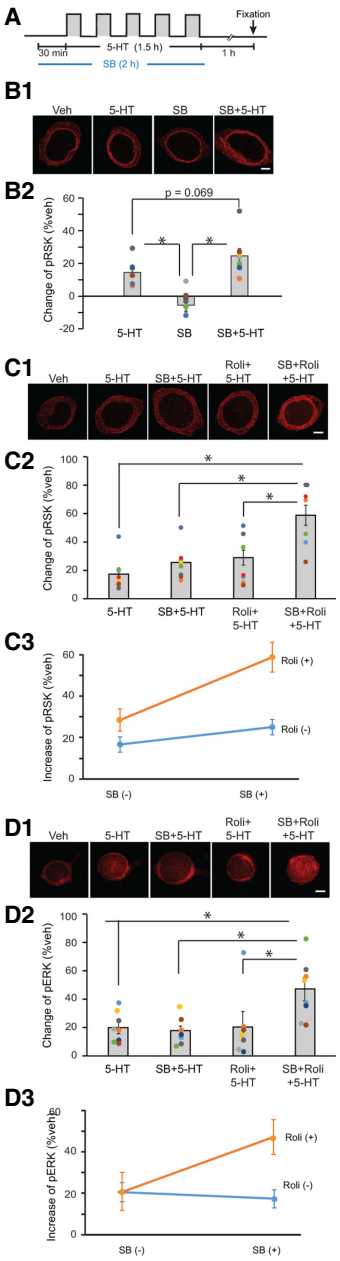

Figure 6. Effects of SB and rolipram on 5-HT-induced increase in pRSK. (*A*) Protocol for standard five pulses of 5-HT treatment in the present of p38 MAPK inhibitor SB 239063 (SB). (*B1*,*B2*) Inhibition of p38 MAPK potentiates 5-HT-induced phosphorylation of RSK. (*B1*) Representative confocal images of pRSK in SNs 1 h after 5-HT treatment with SB. (*B2*) Summary data. SB slightly but not significantly potentiated the 5-HT-induced increase in pRSK. (*C1*–*C3*) Simultaneous activation of PKA and inhibition of p38 MAPK synergistically enhanced RSK activation. (*C1*) Representative confocal images of pRSK in SNs 1 h after 5-HT treatment with SB and/or rolipram. (*C2*) Summary data. SB+Roli potentiated the 5-HT-induced increase in pRSK. (*C3*) Two-way ANOVA revealed that Roli together with SB synergistically potentiated the 5-HT-induced increase in pRSK. (*D1*–*D3*) Simultaneous activation of PKA and inhibition of p38 MAPK synergistically enhanced ERK activation. (*D1*) Representative confocal images of pERK in SNs 1 h after 5-HT treatment with SB and/or rolipram. (*D2*) Summary data. SB+Roli potentiated the 5-HT-induced increase in pERK. (*D3*) Two-way ANOVA revealed that Roli together with SB synergistically potentiated the 5-HT-induced increase in pERK. Different-colored dots in each group indicate individual experiments, and the same color in different groups represents one experiment. Scale bar, 20 µm.

respectively. The increase of pERK in the combined-drug group was 46% ± 7% of control (Fig. 6D2). One-way ANOVA indicated significant overall differences among the groups ($F_{(3,26)} = 4.732$, $P = 0.009$). Post hoc comparisons (SNK) revealed the combined drugs induced a significant increase in pERK compared with the other three groups (SB+Roli+5-HT vs. 5-HT, $q = 4.263$, $P = 0.015$; SB+Roli +5-HT vs. SB+5-HT, $q = 4.554$, $P = 0.017$; SB+Roli+5-HT vs. Roli +5-HT, $q = 4.029$, $P = 0.009$), without significant effects from either SB or rolipram on 5-HT-induced pERK (SB+5-HT vs. 5-HT, $q = 0.435$, $P = 0.761$; Roli+5-HT vs. 5-HT, $q = 0.09$, $P = 0.95$). Importantly, the interaction between rolipram and SB on pERK was significant (two-way ANOVA, $F_{(1,26)} = 4.981$, $P = 0.034$) (Fig. 6D3), indicating the drug combination of SB and rolipram synergistically increased 5-HT-induced phosphorylation of ERK.

Discussion

The reduction in LTF after RSK inhibition suggests *Aplysia* sensory motor neuron cocultures can be a useful cellular system for studying deficits in synaptic plasticity analogous to those associated with CLS.

PKA and ERK activation by pharmacological approaches

Two cascades essential for LTF mediate activation of PKA (Schacher et al. 1988; Muller and Carew 1998; Chain et al. 1999) and of ERK (Michael et al. 1998; Sharma et al. 2003; Sharma and Carew 2004). These kinases phosphorylate transcription factors (CREB1 for PKA, and CREB2 for ERK) (Bartsch et al. 1995, 1998), leading to induction of genes required for LTF (Lee et al. 2006; Alberini 2009). These data suggest that combined pharmacological activation of PKA and ERK may synergistically enhance LTF and LTM. We used rolipram, an inhibitor of cAMP phosphodiesterase (PDE), to activate PKA (Liu et al. 2017), given that PDE4 long and short forms have been identified in *Aplysia* (Park et al. 2005; Kim et al. 2014) and are inhibited by rolipram (Park et al. 2005). The current *Aplysia* transcriptome (Orvis et al. 2022) contains sequences matching two alternatively spliced PDE4 isoforms previously identified (Kim et al. 2014). Rolipram has improved long-term potentiation (LTP) and LTM in normal rodents and in rodent models of Rubinstein–Taybi syndrome and traumatic brain injury (Bourtchouladze et al. 2003; Titus et al. 2013).

We used the DUSP6 inhibitor NSC295642 to activate ERK without activating p38 MAPK (Vogt et al. 2003; Liu et al. 2017). However, NSC295462 might also indirectly inhibit ERK by downregulating Ras, perhaps on a longer time scale, given that NSC295642 can inhibit C-terminal CaaX proteases including Rce1p, which is involved in Ras maturation (Manandhar et al. 2007b, 2010). Although we did not examine the effects of NSC295642 on Ras/Raf activation, we have measured ERK activation after application of NSC295642. 5-HT-mediated phosphorylation/activation of ERK was enhanced (Liu et al. 2017), indicating the net outcome for NSC295642 is to activate ERK in *Aplysia* neurons.

Synergism in rescue of deficits in LTF and in RSK activation

Drug treatment is often accompanied by side effects, such as inhibition of CaaX proteases by NSC295642 (Manandhar et al. 2007a, 2010) as well as possible inhibition of cell migration (Beshir et al. 2008). However, combination therapies have advantages over single drugs since they allow for effectiveness with substantially lower dosages of the individual drugs (Slinker 1998; Barrera et al. 2005; Zimmermann et al. 2007). Our current studies support the idea that drug combinations could capitalize on synergistic interactions resulting from nonlinear properties of the signaling cascades

mediating LTM. This synergism leads to lower doses, which may reduce the side effects of these drugs (Smolen et al. 2014, 2021; Zhang et al. 2014). It is plausible that combined-drug treatments similar to those we have examined could help to rescue deficient synaptic plasticity and memory, such as occurs in CLS, by simultaneously activating signaling pathways that converge onto a target (e.g., CREB1) necessary for long-term synaptic plasticity (Badshah et al. 2015; Cuadrado-Tejedor et al. 2015, 2019; Smolen et al. 2021).

We found that LTF impaired due to RSK inhibition was not restored by single drugs that individually activate either PKA or ERK pathways (Fig. 1). However, the combined drugs at these doses produced a synergistic effect that rescued impaired synaptic plasticity in the CLS model (Figs. 2A2, 3B). This rescue in BID-impaired LTF was accompanied by a synergistic increase in 5-HT-induced phosphorylated RSK (pRSK) in BID-treated SNs (Fig. 4C2,C3). In addition, at these low doses, the drug combination had no adverse effects on basal synaptic strength (Fig. 2B2).

This pRSK increase induced by dual drugs may explain, at least in part, the synergistic rescue of LTF downstream from pRSK. It is also likely that the synergistic rescue of LTF to normal levels depends in part on actions of rolipram and NSC295642 that do not involve RSK, such as enhanced phosphorylation of CREB1 by PKA and enhanced phosphorylation of CREB2 by ERK.

Computational modeling gives insight into determinants of synergism

The model of Zhang et al. (2021) was modified to explore conditions conducive to synergism by systematically simulating the effects of combined drugs on pERK, RSK, and C/EBP. The simulations in this study cannot quantitatively predict the optimal combination of drug concentrations for the synergism of LTF. However, the results provide a qualitative prediction that a PKA activator and p38 MAPK inhibitor together would synergistically enhance LTF.

In this model (Fig. 5A), PKA can activate RSK by two indirect pathways: pathway 10 (Zhang et al. 2021) and pathways $3 \rightarrow 6 \rightarrow 7$ via *Aplysia* neurotrophin (ApNT)/receptor TrkB (Jin et al. 2018; Zhang et al. 2021), thus forming a feed-forward loop. The ERK–p38 MAPK feedback loop suppresses the increase of pERK, reducing activity of RSK (pathways $7 \rightarrow 8 \rightarrow 9 \rightarrow 6 \rightarrow 7$). The PKA and ERK/p38 MAPK cascades thereby interact to regulate the phosphorylation and activities of CREB1 and CREB2, which in turn increases the synthesis and activation of C/EBP, leading to the increased pC/EBP essential for LTF. CREB1 activation also enhances TGF-β expression, which can further activate ERK (Kopec et al. 2015; Shobe et al. 2016). The complex interaction between kinases and transcriptional factors makes it impossible to efficiently design a combined treatment only based on empirical studies. Computational models are essential to gain insights into mechanisms underlying synergism that cannot be achieved by intuition alone.

The model predicted that the negative feedback loop in which RSK activates p38 MAPK activation, which in turn inhibits MEK/ERK/RSK and enhances the repression of C/EBP expression by CREB2, may limit the extent of 5-HT-induced RSK activation (Zhang et al. 2021). Relieving this negative feedback would help exert synergistic effects. With RSK inhibited, this negative feedback loop is weakened. Therefore, the range of potential RSK activation is less limited, which apparently facilitates synergistic interaction of PKA activation and ERK activation (Fig. 5D1,D2).

The model also predicted that a PKA activator combined with a p38 MAPK inhibitor could be another useful drug combination due to their synergistic activation of RSK and LTF (Fig. 5C,D1, D2). In contrast to BID, which suppresses the activation of CREB1 (Fig. 5A, pathway 13), p38 MAPK inhibition suppresses activation of the transcription inhibitor CREB2 (Fig. 5A, pathway 15), further enhancing LTF. Potentiated activation of RSK by a p38 MAPK inhibitor was empirically verified (Fig. 6B2), as was synergistic activation of ERK and RSK by a combination of this inhibitor with rolipram (Fig. 6C2,D2). Taken together, the above results demonstrate ways in which the complex interactions between PKA and MAPK pathways can affect the outcome of combined drugs. The intertwined PKA → RSK feed-forward loop, which promotes synergism, and RSK → p38 MAPK negative feedback loop, which suppresses synergism, together determined the dynamics of kinase and transcription factor activation. Cellular models of disorders that affect synaptic plasticity and learning, such as CLS, may constitute a useful strategy to identify candidate drug combinations to treat aspects of these disorders, and combining biologically realistic computational models with empirical tests of model predictions (Zhang et al. 2011, 2021; Liu et al. 2013, 2020; Zhou et al. 2015) can help explain synergism of drug combinations.

Materials and Methods

Cell culture and pharmacological treatment

Isolated sensory neurons (SNs) or SN–L7 motor neuron (SN-MN) cocultures from *Aplysia californica* (National Institutes of Health *Aplysia* Resource Facility, University of Miami) were prepared according to conventional procedures (Zhang et al. 2011; Liu et al. 2020). The standard 5-HT protocol is to treat SN cultures or SN-MN cocultures with five 5-min pulses of 50 μM 5-HT (Sigma H9523) with a uniform interstimulus interval (ISI) of 20 min (onset to onset) (Zhang et al. 2011). A separate group of control cultures was not treated with 5-HT but was treated with vehicle alone (Veh; L15:ASW) with ISIs of the standard protocol.

BI-D1870 (BID; Santa Cruz Biotechnology CAS 501437-28-1) is a small cell-permeant molecule that specifically inhibits RSKs (Sapkota et al. 2007; Liu et al. 2020). To activate the ERK pathway, we used the DUSP6 inhibitor NSC295642 (Santa Cruz Biotechnology CAS 77111-29-6) (Liu et al. 2017). To activate the PKA pathway, we used rolipram (Sigma R6520) (Liu et al. 2017) but reduced the concentration to 0.1 μM. At this concentration, rolipram can still enhance 5-HT-induced phosphorylation of CREB1 (pCREB1) (see the Supplemental Material). SB 203580 was used to block p38 MAPK activity (Sigma 559389) (Liu et al. 2014). For drug treatment, SNs or cocultures were exposed to drugs for 30 min before and throughout 5-HT treatment. See the Supplemental Material for details.

Immunofluorescence

SNs were starved with a solution of 50% L15 and 50% artificial seawater for 2 h before drug treatment. After repeated 5-HT treatment, SNs were fixed for immunofluorescence at 1 h after treatments, following standard procedures (Chin et al. 1999; Liu et al. 2011, 2020). The specificity of the antibody against phosphorylated p90 RSK (anti-pRSK [Thr573]; Cell Signaling 9346) has been validated (Liu et al. 2020), and this antibody was used in 1:400 dilution. These experiments were performed in a blind manner so that the investigator analyzing the images was unaware of the treatment the SNs received. The number of samples (*n*) reported in the Results indicates the number of dishes assessed.

Electrophysiology

Excitatory postsynaptic potentials (EPSPs) were recorded from MNs from the SN-MN cocultures following established procedures (Liu et al. 2008, 2011, 2013; Zhang et al. 2011; Zhou et al. 2015). The number of samples (*n*) reported in the Results indicates the number of cocultures. All of the above experiments were performed in a blind manner so that the investigator performing the electrophysiology was unaware of the treatment the neurons received.

Statistical analyses

For immunocytochemistry, SNs were isolated from the same animal in each experimental repetition (Figs. 4, 6). When SNs were fixed for immunocytochemistry followed by confocal imaging, the imaging parameters were fixed throughout each experiment repetition. In all cases, immunoreactivities to pRSK in 5-HT or drug treatment groups were normalized to vehicle control, and one-way ANOVA was used on normalized data, followed by the post hoc Student–Newman–Keuls method (SNK) for multiple comparisons analysis (Ormond et al. 2004; Liu et al. 2008, 2011, 2013, 2014, 2017, 2020) . SigmaPlot version 11 (Systat Software, Inc.) was used to perform all statistical analyses.

For electrophysiological experiments, the amplitudes of the EPSPs were assessed before (pretest) and 24 h after (posttest) 5-HT treatment. In contrast to immunofluorescence, these data were normalized for one-way ANOVA analysis, followed by SNK post hoc analysis. Posttest data were normalized to the corresponding measurements made at pretest. To examine possible changes in resting potentials and input resistance of MNs and SNs caused by BID, measurements were made before (pretest) and 24 h after (posttest) vehicle or BID treatment. Student's *t*-test was used to compare the changes [(post-pre)/pre] in the BID group with those in the vehicle group.

To evaluate synergistic effects of dual-drug treatments on LTF and RSK activation, we used a two-way ANOVA to assess the interaction between two treatment factors (Coss et al. 2007; Thackray et al. 2010; Binatti et al. 2021; Ewing et al. 2021; Pantaleon Garcia et al. 2022; Zwolak and Wnuk 2022). The significance of the combined-drug interaction was used to evaluate the null hypothesis that the combined effect of two drugs is merely additive (Figs. 3, 4B3,C3, 6C3,D3).

Data from all experiments are presented as means ± SEM, and $P < 0.05$ was considered to represent statistical significance. All of the experiments were done in a blind manner with the investigators performing the analyses unaware of treatments.

Competing interest statement

The authors declare no competing interests.

Acknowledgments

We thank E. Kartikaningrum for preparing cultures. This study was supported by National Institutes of Health grants NS019895 and NS102490.

Author contributions: R.Y.-L., Y.Z., and J.H.B. contributed to the conception of the study. R.Y.-L. and Y.Z. designed and conducted the experiments and analyzed the results. P.S., L.J.C., and J.H.B. were involved in interpretation of the data and writing of the article. All authors reviewed the manuscript.

References

Alberini CM. 2009. Transcription factors in long-term memory and synaptic plasticity. *Physiol Rev* **89:** 121–145. doi:10.1152/physrev.00017.2008

Alberini CM, Kandel ER. 2014. The regulation of transcription in memory consolidation. *Cold Spring Harb Perspect Biol* **7:** a021741. doi:10.1101/cshperspect.a021741

Alberini CM, Ghirardi M, Metz R, Kandel ER. 1994. *C/EBP* is an immediate-early gene required for the consolidation of long-term facilitation in *Aplysia*. *Cell* **76:** 1099–1114. doi:10.1016/0092-8674(94)90386-7

Badshah H, Ali T, Ahmad A, Kim MJ, Abid NB, Shah SA, Yoon GH, Lee HY, Kim MO. 2015. Co-treatment with anthocyanins and vitamin c ameliorates ethanol-induced neurodegeneration via modulation of GABAB receptor signaling in the adult rat brain. *CNS Neurol Disord Drug Targets* **14:** 791–803. doi:10.2174/1871527314666150225142919

Barrera NP, Morales B, Torres S, Villalon M. 2005. Principles: mechanisms and modeling of synergism in cellular responses. *Trends Pharmacol Sci* **26:** 526–532. doi:10.1016/j.tips.2005.08.003

Bartsch D, Ghirardi M, Skehel PA, Karl KA, Herder SP, Chen M, Bailey CH, Kandel ER. 1995. *Aplysia* CREB2 represses long-term facilitation: relief of repression converts transient facilitation into long-term functional and structural change. *Cell* **83:** 979–992. doi:10.1016/0092-8674(95)90213-9

Bartsch D, Casadio A, Karl KA, Serodio P, Kandel ER. 1998. CREB1 encodes a nuclear activator, a repressor, and a cytoplasmic modulator that form a regulatory unit critical for long-term facilitation. *Cell* **95:** 211–223. doi:10.1016/S0092-8674(00)81752-3

Beshir AB, Guchhait SK, Gascon JA, Fenteany G. 2008. Synthesis and structure-activity relationships of metal-ligand complexes that potently inhibit cell migration. *Bioorg Med Chem Lett* **18:** 498–504. doi:10.1016/j.bmcl.2007.11.099

Binatti E, Zoccatelli G, Zanoni F, Dona G, Mainente F, Chignola R. 2021. Effects of combination treatments with astaxanthin-loaded microparticles and pentoxifylline on intracellular ROS and radiosensitivity of J774A.1 macrophages. *Molecules* **26:** 5152. doi:10.3390/molecules26175152

Bourtchouladze R, Lidge R, Catapano R, Stanley J, Gossweiler S, Romashko D, Scott R, Tully T. 2003. A mouse model of Rubinstein–Taybi syndrome: defective long-term memory is ameliorated by inhibitors of phosphodiesterase 4. *Proc Natl Acad Sci* **100:** 10518–10522. doi:10.1073/pnas.1834280100

Byrne JH, Hawkins RD. 2015. Nonassociative learning in invertebrates. *Cold Spring Harb Perspect Biol* **7:** a021675. doi:10.1101/cshperspect.a021675

Chain DG, Casadio A, Schacher S, Hegde AN, Valbrun M, Yamamoto N, Goldberg AL, Bartsch D, Kandel ER, Schwartz JH. 1999. Mechanisms for generating the autonomous cAMP-dependent protein kinase required for long-term facilitation in *Aplysia*. *Neuron* **22:** 147–156. doi:10.1016/S0896-6273(00)80686-8

Chin J, Angers A, Cleary LJ, Eskin A, Byrne JH. 1999. TGF-β1 in *Aplysia*: role in long-term changes in the excitability of sensory neurons and distribution of TβR-II-like immunoreactivity. *Learn Mem* **6:** 317–330. doi:10.1101/lm.6.3.317

Choi YH, Lee SN, Aoyagi H, Yamasaki Y, Yoo JY, Park B, Shin DM, Yoon HG, Yoon JH. 2011. The extracellular signal-regulated kinase mitogen-activated protein kinase/ribosomal S6 protein kinase 1 cascade phosphorylates cAMP response element-binding protein to induce MUC5B gene expression via D-prostanoid receptor signaling. *J Biol Chem* **286:** 34199–34214. doi:10.1074/jbc.M111.247684

Coss D, Hand CM, Yaphockun KK, Ely HA, Mellon PL. 2007. p38 mitogen-activated protein kinase is critical for synergistic induction of the FSHβ gene by gonadotropin-releasing hormone and activin through augmentation of c-Fos induction and Smad phosphorylation. *Mol Endocrinol* **21:** 3071–3086. doi:10.1210/me.2007-0247

Cuadrado-Tejedor M, Garcia-Barroso C, Sanzhez-Arias J, Mederos S, Rabal O, Ugarte A, Franco R, Pascual-Lucas M, Segura V, Perea G, et al. 2015. Concomitant histone deacetylase and phosphodiesterase 5 inhibition synergistically prevents the disruption in synaptic plasticity and it reverses cognitive impairment in a mouse model of Alzheimer's disease. *Clin Epigenetics* **7:** 108. doi:10.1186/s13148-015-0142-9

Cuadrado-Tejedor M, Perez-Gonzalez M, Garcia-Munoz C, Muruzabal D, Garcia-Barroso C, Rabal O, Segura V, Sanchez-Arias JA, Oyarzabal J, Garcia-Osta A. 2019. Taking advantage of the selectivity of histone deacetylases and phosphodiesterase inhibitors to design better therapeutic strategies to treat Alzheimer's disease. *Front Aging Neurosci* **11:** 149. doi:10.3389/fnagi.2019.00149

Delaunoy JP, Dubos A, Marques Pereira P, Hanauer A. 2006. Identification of novel mutations in the RSK2 gene (RPS6KA3) in patients with Coffin–Lowry syndrome. *Clin Genet* **70:** 161–166. doi:10.1111/j.1399-0004.2006.00660.x

Dufresne SD, Bjorbaek C, El-Haschimi K, Zhao Y, Aschenbach WG, Moller DE, Goodyear LJ. 2001. Altered extracellular signal-regulated kinase signaling and glycogen metabolism in skeletal muscle from p90 ribosomal S6 kinase 2 knockout mice. *Mol Cell Biol* **21:** 81–87. doi:10.1128/MCB.21.1.81-87.2001

Ewing ST, Dorcely C, Maidi R, Paker G, Schelbaum E, Ranaldi R. 2021. Low-dose polypharmacology targeting dopamine D1 and D3 receptors reduces cue-induced relapse to heroin seeking in rats. *Addict Biol* **26:** e12988. doi:10.1111/adb.12988

Finkbeiner S, Tavazoie SF, Maloratsky A, Jacobs KM, Harris KM, Greenberg ME. 1997. CREB: a major mediator of neuronal neurotrophin responses. *Neuron* **19:** 1031–1047. doi:10.1016/S0896-6273(00)80395-5

Fonseca BD, Alain T, Finestone LK, Huang BP, Rolfe M, Jiang T, Yao Z, Hernandez G, Bennett CF, Proud CG. 2011. Pharmacological and genetic evaluation of proposed roles of mitogen-activated protein kinase/extracellular signal-regulated kinase kinase (MEK), extracellular signal-regulated kinase (ERK), and p90(RSK) in the control of mTORC1 protein signaling by phorbol esters. *J Biol Chem* **286:** 27111–27122. doi:10.1074/jbc.M111.260794

Guan Z, Giustetto M, Lomvardas S, Kim JH, Miniaci MC, Schwartz JH, Thanos D, Kandel ER. 2002. Integration of long-term-memory-related synaptic plasticity involves bidirectional regulation of gene expression and chromatin structure. *Cell* **111:** 483–493. doi:10.1016/S0092-8674(02)01074-7

Guan Z, Kim JH, Lomvardas S, Holick K, Xu S, Kandel ER, Schwartz JH. 2003. p38 MAP kinase mediates both short-term and long-term synaptic

depression in *Aplysia*. *J Neurosci* **23:** 7317–7325. doi:10.1523/JNEUROSCI.23-19-07317.2003
Jin I, Udo H, Nicholls R, Zhu H, Kandel ER, Hawkins RD. 2018. Autocrine signaling by an *Aplysia* neurotrophin forms a presynaptic positive feedback loop. *Proc Natl Acad Sci* **115:** E11168–E11177. doi:10.1073/pnas.1808600115
Kim KH, Jun YW, Park Y, Lee JA, Suh BC, Lim CS, Lee YS, Kaang BK, Jang DJ. 2014. Intracellular membrane association of the *Aplysia* cAMP phosphodiesterase long and short forms via different targeting mechanisms. *J Biol Chem* **289:** 25797–25811. doi:10.1074/jbc.M114.572222
Kopec AM, Philips GT, Carew TJ. 2015. Distinct growth factor families are recruited in unique spatiotemporal domains during long-term memory formation in *Aplysia californica*. *Neuron* **86:** 1228–1239. doi:10.1016/j.neuron.2015.04.025
Lee JA, Lee SH, Lee C, Chang DJ, Lee Y, Kim H, Cheang YH, Ko HG, Lee YS, Jun H, et al. 2006. PKA-activated ApAF-ApC/EBP heterodimer is a key downstream effector of ApCREB and is necessary and sufficient for the consolidation of long-term facilitation. *J Cell Biol* **174:** 827–838. doi:10.1083/jcb.200512066
Liu RY, Fioravante D, Shah S, Byrne JH. 2008. cAMP response element-binding protein 1 feedback loop is necessary for consolidation of long-term synaptic facilitation in *Aplysia*. *J Neurosci* **28:** 1970–1976. doi:10.1523/JNEUROSCI.3848-07.2008
Liu RY, Cleary LJ, Byrne JH. 2011. The requirement for enhanced CREB1 expression in consolidation of long-term synaptic facilitation and long-term excitability in sensory neurons of *Aplysia*. *J Neurosci* **31:** 6871–6879. doi:10.1523/JNEUROSCI.5071-10.2011
Liu RY, Zhang Y, Baxter DA, Smolen P, Cleary LJ, Byrne JH. 2013. Deficit in long-term synaptic plasticity is rescued by a computationally predicted stimulus protocol. *J Neurosci* **33:** 6944–6949. doi:10.1523/JNEUROSCI.0643-13.2013
Liu RY, Zhang Y, Coughlin BL, Cleary LJ, Byrne JH. 2014. Doxorubicin attenuates serotonin-induced long-term synaptic facilitation by phosphorylation of p38 mitogen-activated protein kinase. *J Neurosci* **34:** 13289–13300. doi:10.1523/JNEUROSCI.0538-14.2014
Liu RY, Neveu C, Smolen P, Cleary LJ, Byrne JH. 2017. Superior long-term synaptic memory induced by combining dual pharmacological activation of PKA and ERK with an enhanced training protocol. *Learn Mem* **24:** 289–297. doi:10.1101/lm.044834.116
Liu RY, Zhang Y, Smolen P, Cleary LJ, Byrne JH. 2020. Role of p90 ribosomal S6 kinase in long-term synaptic facilitation and enhanced neuronal excitability. *Sci Rep* **10:** 608. doi:10.1038/s41598-020-57484-y
Manandhar S, Cho JM, Kim JA, Kensler TW, Kwak MK. 2007a. Induction of Nrf2-regulated genes by 3H-1, 2-dithiole-3-thione through the ERK signaling pathway in murine keratinocytes. *Eur J Pharmacol* **577:** 17–27. doi:10.1016/j.ejphar.2007.08.018
Manandhar SP, Hildebrandt ER, Schmidt WK. 2007b. Small-molecule inhibitors of the Rce1p CaaX protease. *J Biomol Screen* **12:** 983–993. doi:10.1177/1087057107307226
Manandhar SP, Hildebrandt ER, Jacobsen WH, Santangelo GM, Schmidt WK. 2010. Chemical inhibition of CaaX protease activity disrupts yeast Ras localization. *Yeast* **27:** 327–343. doi:10.1002/yea.1756
Michael D, Martin KC, Seger R, Ning MM, Baston R, Kandel ER. 1998. Repeated pulses of serotonin required for long-term facilitation activate mitogen-activated protein kinase in sensory neurons of *Aplysia*. *Proc Natl Acad Sci* **95:** 1864–1869. doi:10.1073/pnas.95.4.1864
Mohamed HA, Yao W, Fioravante D, Smolen PD, Byrne JH. 2005. cAMP-response elements in *Aplysia creb1, creb2*, and *Ap-uch* promoters: implications for feedback loops modulating long term memory. *J Biol Chem* **280:** 27035–27043. doi:10.1074/jbc.M502541200
Montarolo PG, Goelet P, Castellucci VF, Morgan J, Kandel ER, Schacher S. 1986. A critical period for macromolecular synthesis in long-term heterosynaptic facilitation in *Aplysia*. *Science* **234:** 1249–1254. doi:10.1126/science.3775383
Morice E, Farley S, Poirier R, Dallerac G, Chagneau C, Pannetier S, Hanauer A, Davis S, Vaillend C, Laroche S. 2013. Defective synaptic transmission and structure in the dentate gyrus and selective fear memory impairment in the *Rsk2* mutant mouse model of Coffin–Lowry syndrome. *Neurobiol Dis* **58:** 156–168. doi:10.1016/j.nbd.2013.05.016
Mozzachiodi R, Byrne JH. 2010. More than synaptic plasticity: role of nonsynaptic plasticity in learning and memory. *Trends Neurosci* **33:** 17–26. doi:10.1016/j.tins.2009.10.001
Muller U, Carew TJ. 1998. Serotonin induces temporally and mechanistically distinct phases of persistent PKA activity in *Aplysia* sensory neurons. *Neuron* **21:** 1423–1434. doi:10.1016/S0896-6273(00)80660-1
Ormond J, Hislop J, Zhao Y, Webb N, Vaillaincourt F, Dyer JR, Ferraro G, Barker P, Martin KC, Sossin WS. 2004. ApTrkl, a Trk-like receptor, mediates serotonin-dependent ERK activation and long-term facilitation in *Aplysia* sensory neurons. *Neuron* **44:** 715–728. doi:10.1016/j.neuron.2004.11.001
Orvis J, Albertin CB, Shrestha P, Chen S, Zheng M, Rodriguez CJ, Tallon LJ, Mahurkar A, Zimin AV, Kim M, et al. 2022. The evolution of synaptic and cognitive capacity: insights from the nervous system transcriptome of *Aplysia*. *Proc Natl Acad Sci* **119:** e2122301119. doi:10.1073/pnas.2122301119
Pantaleon Garcia J, Kulkarni VV, Reese TC, Wali S, Wase SJ, Zhang J, Singh R, Caetano MS, Kadara H, Moghaddam SJ, et al. 2022. OBIF: an omics-based interaction framework to reveal molecular drivers of synergy. *NAR Genom Bioinform* **4:** lqac028. doi:10.1093/nargab/lqac028
Park H, Lee JA, Lee C, Kim MJ, Chang DJ, Kim H, Lee SH, Lee YS, Kaang BK. 2005. An Aplysia type 4 phosphodiesterase homolog localizes at the presynaptic terminals of *Aplysia* neuron and regulates synaptic facilitation. *J Neurosci* **25:** 9037–9045. doi:10.1523/JNEUROSCI.1989-05.2005
Poirier R, Jacquot S, Vaillend C, Soutthiphong AA, Libbey M, Davis S, Laroche S, Hanauer A, Welzl H, Lipp HP, et al. 2007. Deletion of the Coffin-Lowry syndrome gene *Rsk2* in mice is associated with impaired spatial learning and reduced control of exploratory behavior. *Behav Genet* **37:** 31–50. doi:10.1007/s10519-006-9116-1
Rawashdeh O, Jilg A, Maronde E, Fahrenkrug J, Stehle JH. 2016. Period1 gates the circadian modulation of memory-relevant signaling in mouse hippocampus by regulating the nuclear shuttling of the CREB kinase pP90RSK. *J Neurochem* **138:** 731–745. doi:10.1111/jnc.13689
Sapkota GP, Cummings L, Newell FS, Armstrong C, Bain J, Frodin M, Grauert M, Hoffmann M, Schnapp G, Steegmaier M, et al. 2007. BI-D1870 is a specific inhibitor of the p90 RSK (ribosomal S6 kinase) isoforms *in vitro* and *in vivo*. *Biochem J* **401:** 29–38. doi:10.1042/BJ20061088
Schacher S, Castellucci VF, Kandel ER. 1988. cAMP evokes long-term facilitation in *Aplysia* sensory neurons that requires new protein synthesis. *Science* **240:** 1667–1669. doi:10.1126/science.2454509
Sharma SK, Carew TJ. 2004. The roles of MAPK cascades in synaptic plasticity and memory in *Aplysia*: facilitatory effects and inhibitory constraints. *Learn Mem* **11:** 373–378. doi:10.1101/lm.81104
Sharma SK, Sherff CM, Shobe J, Bagnall MW, Sutton MA, Carew TJ. 2003. Differential role of mitogen-activated protein kinase in three distinct phases of memory for sensitization in *Aplysia*. *J Neurosci* **23:** 3899–3907. doi:10.1523/JNEUROSCI.23-09-03899.2003
Shobe J, Philips GT, Carew TJ. 2016. Transforming growth factor β recruits persistent MAPK signaling to regulate long-term memory consolidation in *Aplysia californica*. *Learn Mem* **23:** 182–188. doi:10.1101/lm.040915.115
Slinker BK. 1998. The statistics of synergism. *J Mol Cell Cardiol* **30:** 723–731. doi:10.1006/jmcc.1998.0655
Smolen P, Baxter DA, Byrne JH. 2014. Simulations suggest pharmacological methods for rescuing long-term potentiation. *J Theor Biol* **360:** 243–250. doi:10.1016/j.jtbi.2014.07.006
Smolen P, Wood MA, Baxter DA, Byrne JH. 2021. Modeling suggests combined-drug treatments for disorders impairing synaptic plasticity via shared signaling pathways. *J Comput Neurosci* **49:** 37–56. doi:10.1007/s10827-020-00771-4
Thackray VG, Mellon PL, Coss D. 2010. Hormones in synergy: regulation of the pituitary gonadotropin genes. *Mol Cell Endocrinol* **314:** 192–203. doi:10.1016/j.mce.2009.09.003
Titus DJ, Sakurai A, Kang Y, Furones C, Jergova S, Santos R, Sick TJ, Atkins CM. 2013. Phosphodiesterase inhibition rescues chronic cognitive deficits induced by traumatic brain injury. *J Neurosci* **33:** 5216–5226. doi:10.1523/JNEUROSCI.5133-12.2013
Vogt A, Cooley KA, Brisson M, Tarpley MG, Wipf P, Lazo JS. 2003. Cell-active dual specificity phosphatase inhibitors identified by high-content screening. *Chem Biol* **10:** 733–742. doi:10.1016/S1074-5521(03)00170-4
Xing J, Ginty DD, Greenberg ME. 1996. Coupling of the RAS–MAPK pathway to gene activation by RSK2, a growth factor-regulated CREB kinase. *Science* **273:** 959–963. doi:10.1126/science.273.5277.959
Xing J, Kornhauser JM, Xia Z, Thiele EA, Greenberg ME. 1998. Nerve growth factor activates extracellular signal-regulated kinase and p38 mitogen-activated protein kinase pathways to stimulate CREB serine 133 phosphorylation. *Mol Cell Biol* **18:** 1946–1955. doi:10.1128/MCB.18.4.1946
Zhang Y, Liu RY, Heberton GA, Smolen P, Baxter DA, Cleary LJ, Byrne JH. 2011. Computational design of enhanced learning protocols. *Nat Neurosci* **15:** 294–297. doi:10.1038/nn.2990
Zhang Y, Smolen P, Baxter DA, Byrne JH. 2014. Computational analyses of synergism in small molecular network motifs. *PLoS Comput Biol* **10:** e1003524. doi:10.1371/journal.pcbi.1003524
Zhang G, Vilim FS, Liu DD, Romanova EV, Yu K, Yuan WD, Xiao H, Hummon AB, Chen TT, Alexeeva V, et al. 2017. Discovery of leucokinin-like neuropeptides that modulate a specific parameter of feeding motor programs in the molluscan model, *Aplysia*. *J Biol Chem* **292:** 18775–18789. doi:10.1074/jbc.M117.795450
Zhang Y, Smolen PD, Cleary LJ, Byrne JH. 2021. Quantitative description of the interactions among kinase cascades underlying long-term plasticity

of *Aplysia* sensory neurons. *Sci Rep* **11:** 14931. doi:10.1038/s41598-021-94393-0

Zhou L, Zhang Y, Liu RY, Smolen P, Cleary LJ, Byrne JH. 2015. Rescue of impaired long-term facilitation at sensorimotor synapses of *Aplysia* following siRNA knockdown of CREB1. *J Neurosci* **35:** 1617–1626. doi:10.1523/JNEUROSCI.3330-14.2015

Zimmermann GR, Lehar J, Keith CT. 2007. Multi-target therapeutics: when the whole is greater than the sum of the parts. *Drug Discov Today* **12:** 34–42. doi:10.1016/j.drudis.2006.11.008

Zwolak I, Wnuk E. 2022. Effects of sodium pyruvate on vanadyl sulphate-induced reactive species generation and mitochondrial destabilisation in CHO-K1 cells. *Antioxidants* **11:** 909. doi:10.3390/antiox11050909

Received July 5, 2022; accepted in revised form October 24, 2022.